


# HER2 and HLA-A\*02 dual CAR-T cells utilize LOH in a NOT logic gate to address on-target off-tumor toxicity

David Bassan,<sup>1</sup> Leehee Weinberger,<sup>1</sup> Jason Yi,<sup>2</sup> Tanya Kim,<sup>2</sup> Michael R Weist,<sup>2</sup> Gregor B Adams,<sup>2</sup> Orit Foord,<sup>2</sup> Neta Chaim,<sup>1</sup> Sarit Tabak,<sup>1</sup> Nir Bujanover,<sup>1</sup> Yael Lopesco,<sup>1</sup> Kristina Vucci,<sup>2</sup> Caitlin Schnair,<sup>2</sup> Limor Levy-Knafo,<sup>1</sup> Richard L Kendall,<sup>2</sup> Frank J Calzone,<sup>2</sup> Adi Sharbi-Yunger <sup>1</sup>

**To cite:** Bassan D, Weinberger L, Yi J, *et al.* HER2 and HLA-A\*02 dual CAR-T cells utilize LOH in a NOT logic gate to address on-target off-tumor toxicity. *Journal for ImmunoTherapy of Cancer* 2023;**11**:e007426. doi:10.1136/jitc-2023-007426

► Additional supplemental material is published online only. To view, please visit the journal online (<http://dx.doi.org/10.1136/jitc-2023-007426>).

DB, LW and JY contributed equally.

Accepted 14 November 2023



© Author(s) (or their employer(s)) 2023. Re-use permitted under CC BY-NC. No commercial re-use. See rights and permissions. Published by BMJ.

<sup>1</sup>Research, ImmPACT-Bio, Rehovot, Israel

<sup>2</sup>Research, ImmPACT-Bio US, West Hills, California, USA

## Correspondence to

Dr Adi Sharbi-Yunger; [adi@immcompact-bio.com](mailto:adi@immcompact-bio.com)

## ABSTRACT

**Background** One of the major challenges in chimeric antigen receptor (CAR)-T cell therapy for solid tumors is the potential for on-target off-tumor toxicity due to the expression of CAR tumor antigens in essential tissues and organs. Here, we describe a dual CAR NOT gate incorporating an inhibitory CAR (iCAR) recognizing HLA-A\*02 (“A2”) that enables effective treatment with a potent HER2 activating CAR (aCAR) in the context of A2 loss of heterozygosity (LOH).

**Methods** A CAR-T cell screen was conducted to identify inhibitory domains derived from natural immune receptors (iDomains) to be used in a NOT gate, to kill A2<sup>-</sup> HER2<sup>+</sup> lung cancer cell lines but spare A2<sup>+</sup> HER2<sup>+</sup> lung cancer cell-lines with high specificity. The extensive analysis of lead candidates included T-cell activation and killing, assays of reversibility and durability in sequential challenges, target cell specificity in mixed 3D spheroids and 2D cultures, and the characterization of CAR expression level and cell-trafficking.

**Results** A leukocyte immunoglobulin-like receptor B1 (LIR1) iDomain iCAR was identified as most effective in regulating the cytotoxicity of a second generation HER2 aCAR. Target transfer experiments demonstrated that the ‘on’ and ‘off’ cell state of the LIR1 NOT gate CAR-T cell is both durable and reversible. Protection required iCAR signaling and was associated with reduced aCAR and iCAR surface expression. iCAR regulation was sufficient to generate high target specificity in a 3D adjacent spheroid assay designed to model the interface between clonal A2 LOH foci and normal tissue. However, we observed significant bystander killing of A2<sup>+</sup> cells in admix culture through aCAR dependent and independent mechanisms. LIR1 NOT gate CAR-T cells conferred protection against H1703-A2<sup>+</sup> tumors and high efficacy against H1703-A2<sup>-</sup> tumors in-vivo. We observed that the iCAR is inactive in A2<sup>+</sup> donors due to cis-binding, but Clustered Regularly Interspaced Short Palindromic Repeats (CRISPR) knockout of HLA-A fully restored iCAR activity.

**Conclusions** We have preclinically validated an iCAR NOT gate technology broadly applicable for targeting HER2 expression in the context of A2 LOH. This approach is designed to prevent off tumor toxicity while allowing highly potent antitumor activity.

## WHAT IS ALREADY KNOWN ON THIS TOPIC

⇒ On-target toxicity due to the expression of chimeric antigen receptor (CAR) tumor antigens in vital organs is a significant barrier for the clinical translation of chimeric antigen receptor T (CAR-T) cell therapy to solid tumors.

## WHAT THIS STUDY ADDS

⇒ We have shown preclinically that an inhibitory CAR (iCAR) recognizing HLA-A\*02 can be used to develop a NOT gate dual CAR-T cell that enables potent targeting of low/normal HER2 expression with an efficient second-generation activating CAR in the context of HLA-A\*02 loss-of-heterozygosity (LOH) while simultaneously protecting normal cells.

## HOW THIS STUDY MIGHT AFFECT RESEARCH, PRACTICE OR POLICY

⇒ Our iCAR LOH targeting technology is applicable to a wide range of solid tumor types where chromosomal instability is common. The self-regulation imposed by the iCAR on conventional CAR-T addresses cytokine release syndrome and T-cell exhaustion in addition to tumor specificity.

## INTRODUCTION

Cellular immunotherapy using CD19-targeted chimeric antigen receptor T (CAR-T) cells has achieved unprecedented outcomes for patients with relapsed or refractory lymphoma including durable complete responses in approximately 40%–60% of aggressive lymphomas, and 60%–80% in Acute Lymphoblastic Leukemia (ALL).<sup>1</sup> However, CAR-T treatment for solid tumors requires more sophisticated engineering approaches since CAR tumor antigens are expressed on normal cells, resulting in ‘on-target, off-tumor’ toxicity.<sup>2</sup> The lack of tumor specificity due to the wide expression of HER2 on normal tissues and tumors, often at similar levels, is a fundamental barrier

for effective HER2-targeted CAR-T treatment. Indeed, HER2 expression in normal tissues led to fatal toxicities following HER2 CAR-T infusion.<sup>3,4</sup>

Logic gates incorporating multiple cell-surface targets and rewired T-cell regulatory circuits offer a new opportunity to augment CAR-T selectivity.<sup>5-7</sup> We have taken a NOT gate approach to develop a method to target HER2<sup>+</sup> cancers specifically in the context of A2 loss of heterozygosity (LOH). The NOT gate is a dual CAR system composed of an inhibitory CAR (iCAR) that inhibits T-cell activation, and an aCAR (activating CAR) responsible for T-cell activation and killing. The iCAR binding is A2 allele-specific, whereas the aCAR recognizes all HER2 germline variants. Engagement of the iCAR in normal tissues activates acute inhibitory pathways that suppress T-cell activation. Loss of A2 (iCAR target) expression in tumors of heterozygous individuals (LOH) enables aCAR activation and HER2-targeted killing. HER2 amplification, transcriptional overexpression or HER2 mutation are not essential since it is A2 LOH that generates irreversible tumor specificity.

The A2 allele was selected to validate the LOH NOT gate concept for several reasons. Approximately 45% of humans are A2 heterozygotes (Allele Frequency Net Database - AFND, <http://allelefrequencies.net>) and HLA-A is expressed in all normal tissues. The frequency of early HLA-A LOH in a broad range of solid tumors conservatively centers about 13% and generally encompasses the complete histocompatibility locus as a result of whole chromosome 6 or 6p aneuploidy.<sup>8-15</sup> The increased presence of HLA-I LOH in metastatic lung cancer suggests that HLA-I loss is positively selected as an immune escape mechanism during tumor progression.<sup>12,15</sup>

The concept for targeting loss-of-gene expression with CAR-T cells was first validated using a Programmed Cell Death Protein 1 (PD1) iDomain and Prostate-specific membrane antigen (PSMA) as an iCAR target.<sup>16</sup> More recently, the results obtained with PD1 have been confirmed in other iCAR NOT gate publications,<sup>17,18</sup> and extended to new iDomains<sup>19</sup>; and leukocyte immunoglobulin-like receptor B1 (LIR1).<sup>20-22</sup> In this study, we have conducted an unbiased screen to identify iDomains capable of regulating a potent HER2 aCAR targeting low/normal HER2 expression. The screen identified several members of the greater NK receptor family as having development potential. We provide evidence suggesting that an A2-directed iCAR NOT gate incorporating a LIR1 signaling domain may enable safe and effective targeting of normal HER2 expression in the context of A2 LOH. HER2 amplification or overexpression is not required. Our study highlights the possible clinical utility to address cytokine release syndrome (CRS), T-cell exhaustion and LOH tumor heterogeneity.

## METHODS

### Cell lines

Cells lines were maintained in RPMI-1640 containing 2 mM L-glutamine (Sartorius) supplemented with 10% heat-inactivated Fetal Bovine Serum (FBS) (Sigma-Aldrich),

1 mM Sodium pyruvate (Sartorius), 100 U/mL penicillin and 0.1 mg/mL streptomycin (Sigma-Aldrich), and regularly tested using Mycoalert detection kit (Lonza). The genetically modified cell lines generated for this study are listed in online supplemental table S1. H1650 and H1703 cells were transduced with Firefly Luciferase Lentiviruses (BPS Bioscience), selected with 800 µg/mL G418 and maintained in 200 µg/mL. Luc-labeled cells were transduced with NuLight Green ('GFP') or Red Lentiviruses ('RFP') (Sartorius) and selected with Puromycin, 0.5 µg/mL for H1650 or 2 µg/mL for H1703. HLA-A editing used sgRNA CRISPR1097726\_SGM (Thermo-Fisher) with TrueCut Cas9 Protein v (Cas9) (Thermo-Fisher), and CRISPRMAX (Thermo-Fisher) according to manufacturer's protocol. CRISPR editing with HER2 (ERBB2) sgRNA (TCATCGCTCACAAACCAAGTG, Synthego) was performed using TrueCut Cas9 Protein v (Thermo-Fisher) using a ECM830 (BTX) electroporation system. HER2-edited cells were enriched by negative selection with anti-HER2-PE (Miltenyi Biotec), PE magnetic beads (Miltenyi Biotec) and MS columns (Miltenyi Biotec). H1650-A2<sup>+</sup> CD19<sup>+</sup> Luc-GFP cells, cells were generated by transduction with CD19 lentivirus (Vector Builder) and selected with 10 µg/mL blasticidin.

### Flow cytometry

CAR-T samples were collected from cocultures following addition of Phosphate-buffered saline (PBS)+ 10 mM EDTA (Biological industries) for 1 min. Cells were stained and analyzed according to standard flow cytometry protocols at 4°C for 30 min in PBS (Sartorius)+ 2% FBS (Sigma-Aldrich) using a Celesta (BD) or Attune NxT (Invitrogen) cytometer. The Fluorescence-activated cell sorting (FACS) antibodies are listed in online supplemental table S1. Dead cells were identified by 4',6-diamidino-2-phenylindole (DAPI) (Sigma-Aldrich) staining. Analysis was performed using FlowJo v10.8 Software (BD Life Sciences). For cell surface receptor quantification, cells were stained with Flag-APC, cMyc-FITC, Tet-PE or anti-trastuzumab+anti-human-APC. Quantum MESF beads and Quantum Simply Cellular beads (Bangs Laboratories) were used according to manufacturer recommendations. For iCAR quantification, tetramer Median Fluorescence Intensity (MFI) was calibrated using Jurkat cells stably expressing cMyc-tagged iCAR, that were stained with both Tetramer and cMyc. Cell-surface HLA-A2 and HER2 expression was quantified using anti-HER2 PE (Miltenyi Biotec, 1:5) and anti-HLA-A2 APC (Thermo Fisher, 1:10).

### CAR-T cells

Frozen healthy donor peripheral blood mononuclear cell (PBMCs; HemaCare, US; Israel Blood Bank), enriched using Ficol-Paque PLUS (Sigma-Aldrich), were thawed in 96-well plates at 1E6 cells/ml in LymphoOne (Takara Bio) plus 1:100 TransAct (Miltenyi Biotec) and 100 U/mL IL-2 (Miltenyi Biotec). Lentiviral vectors generated by VectorBuilder (Guangzhou, China) or Alstem (Richmond, CA) were added (VR33 MOI 10, iCAR NOT gate

MOI 20) on day 1 post-thaw, and transferred to 24 or 6 well G-Rex plates on day 4 in LymphoOne+1% human serum (Miltenyi Biotec) + 100 U/mL IL2 (CAR-T Culture media). IL-2 was replenished on day 6. Unless otherwise noted, NOT gate CAR-T cells were enriched on day 7 using PE-labeled HLA-A2 tetramers and anti-PE microbeads and LS columns according to manufacturer's protocol (Miltenyi Biotec). Enriched cells and controls were reactivated using 1:100 TransAct (1E6 cells/ml). Fresh medium was added on day 8, IL2 replenished on day 10 or 11, and medium replaced on day 12. Cells were harvested for functional assay or frozen in CryoStor CS10 (Biolife solutions) on day 14. Fresh and frozen CAR-T cells were used interchangeably in in-vitro experiments after passing an H1703-Luc A2<sup>+</sup>/A2<sup>-</sup> killing test; acceptance criteria were <20% loss of potency and <20% loss of protection. For A2<sup>+</sup> donors, CRISPR editing was performed on day 2 with sgRNA TACCACCAGTACGCCTACGA (#150, Synthego) at a 4:1 Cas9: sgRNA ratio using a Neon Transfection System (electroporation program #24) with 1-3E6 CAR-T cells in 100  $\mu$ L of buffer T. The cells were subsequently seeded at 1E6 cells/ml in expansion medium on 24-well plates and A2<sup>+</sup> T cells were depleted on day 5 using APC-labeled anti-HLA-A2-APC antibody (Thermo Fisher) with anti-APC microbeads and MS columns. The A2-depleted T cells were seeded in G-Rex plates, in CAR-T culture media without reactivation and iCAR/aCAR positive CAR-T cells were enriched on day 8 using cMyc-FITC, anti-FITC microbeads and LS columns, and expanded similarly to the A2<sup>-</sup> donor protocol.

#### Luciferase (Luc) killing and interferon (IFN)- $\gamma$ assays

Luc-labeled target cells were seeded in 96-well plates (1.0E4 per well) and CAR-T cells were added after 6 hours in duplicate as indicated in the Results section. Following 18 hours incubation and removal of 80  $\mu$ L of supernatant for cytokine assays, the luciferase activity was determined with the Bio-Glo Luciferase Assay system (Promega). Viability was normalized to the maximum RLU signal for a given effector. EC<sub>50</sub> was estimated using GraphPad Prism (Sigmoidal (4PL)). Protection ratio was calculated as A2<sup>+</sup><sub>EC50</sub>/A2<sup>-</sup><sub>EC50</sub>. Unless otherwise noted, CAR-T were prepared with A2<sup>-</sup> donors, and NOT gate CAR-T cells were iCAR enriched. Secreted IFN- $\gamma$  was measured by human IFN- $\gamma$  CBA Flex Set (BD Biosciences) in V-bottom nonbinding 96-well plates (Greiner Bio-One).

#### IncuCyte 2D assay

RFP or GFP-labeled cells, or a mixture (admix) at indicated ratios, were seeded in 96-well plates (Thermo Fisher), 6E3 cells/well, and allowed to adhere overnight. CAR-T cells were added at an E:T ratio of 4:1 unless otherwise noted. The cells were monitored using an IncuCyte S3 with a  $\times$ 10 objective in triplicate and raw image analysis was performed with IncuCyte Software (v2019B). Target cell growth was captured as total green or red intensity and normalized relative to T<sub>0</sub> and inhibition of target

growth relative to the non-transduced (NTD) control as follows: %killing =  $100 \times \left( \frac{\text{NTD}_{\text{Tx}}}{\text{NTD}_{\text{T0}}} - \frac{\text{CAR}_{\text{Tx}}}{\text{CAR}_{\text{T0}}} \right) / \left( \frac{\text{NTD}_{\text{Tx}}}{\text{NTD}_{\text{T0}}} \right)$

The AUC for target cell killing relative to NTD control was determined using GraphPad Prism. To simultaneously monitor apoptosis, IncuCyte Annexin-V Red Reagent (Sartorius) was added prior to effectors and percent killing estimated as the number of Annexin<sup>+</sup> GFP<sup>+</sup> cells divided by total GFP<sup>+</sup> cells.

#### IncuCyte spheroids assay

Individual or admix spheroids were prepared by seeding RFP H1650-A2<sup>+</sup> and GFP H1650-A2<sup>-</sup> cells (3–8 replicates) at 1:1 ratio in 96-well ultralow round attachment plates (Corning) (2.5E3 cells/well) followed by centrifugation at 100g for 10 min. Spheroids developed over 4 days. To form adjacent spheroids, individual RFP H1650-A2<sup>+</sup> and GFP H1650-A2<sup>-</sup> spheroids were combined in a new plate with fresh LymphoOne plus 1% HS using a wide bore pipet tip. The interface between RFP A2<sup>+</sup> and GFP A2<sup>-</sup> spheroids formed spontaneously. CAR-T cells were added, 5E3 cells/well, and monitored using an IncuCyte S3 with a  $\times$ 10 objective. Images were analyzed with IncuCyte Spheroid analysis software module (Sartorius) and %killing based on inhibition of growth was calculated in the same manner as 2D assays.

#### Reversibility and repeated antigen challenge

GFP-labeled H1650-A2<sup>+</sup> or H1650-A2<sup>-</sup> targets were seeded in 10 cm<sup>2</sup> plates, 2E6 cells/plate, and allowed to adhere for 6 hours. CAR-T cells were added at a 1.5:1 E:T ratio and cocultured for 48 hours. For repeated challenges, suspended T cells were collected from the coculture plate and combined with adherent T-cells released by brief treatment (1 min) with PBS 0.5% Bovine Serum Albumin (BSA) plus 10 mM EDTA. H1650 targets were removed using PE-conjugated anti-E cadherin (1:50, Miltenyi Biotec) and anti-P-cadherin antibodies (1:5, R&D Systems) and an EasySep Human PE Position Selection Kit II (StemCell) according to manufacturer protocol. The antigen-stimulated CAR-T cells (6E3 targets cells/well, 1.8E4 or 9E3 CAR-T at 3:1 and 1.5:1 E:T ratio) were then immediately applied to a new culture of either the same H1650 target cells to test durability, or the opposite target cells to test reversibility. Cell apoptosis and growth inhibition were monitored by IncuCyte imaging for 96 hours.

#### Murine xenografts

In-vivo experiments were conducted at Labcorp managed under the Labcorp Institutional Animal Care and Use Committee policies. Female NOD.Cg-Prkdc<sup>scid</sup> Il2rg<sup>tm1Wjl</sup>/SzJ (NSG) mice aged 6–7 weeks (The Jackson Laboratories) were injected subcutaneously with 5E6 of either H1703-A2<sup>+</sup> or H1703-A2<sup>-</sup> cells in a 50% Matrigel solution (Sigma-Aldrich). After tumor implants reached 75–150 mm<sup>3</sup> (V=L  $\times$  W  $\times$  W/2, approximately 12 days), T cells were injected by the tail vein at doses of 1.5E6 to 5E6 CAR-T cells in 200  $\mu$ L of PBS



vehicle. Tumor growth and survival were monitored for up to 50 days post implantation and animals were removed from the study when tumor burden  $>2000 \text{ mm}^3$  or a humane endpoint was reached. Retro-orbital blood samples were collected weekly starting at day 8 into  $\text{K}_2\text{EDTA}$  microtubes and shipped overnight at 24 hours post injection. On receipt of the blood samples,  $30 \mu\text{L}$  was removed from each tube for no-spin, no-wash flow analyses. Briefly, blood was Fc blocked using TruStain Monocyte Blocker (Biolegend) for 5 min and stained with an antibody mix of hCD3-APC-Cy7, hCD8-PE-Cy7 and hCD4-PerCP-Cy5.5 (Biolegend) for 20 min at ambient temperature. Red blood cells were lysed using ACK lysis buffer (Lonza) for 15 min. CountBright Absolute Counting Beads (Thermo-Fisher) were added and samples analyzed on Attune NxT. Absolute cell count = experimental cell count \* (Absolute bead counts / experimental bead count). Samples were analyzed by FlowJo v10.8 Software (BD Life Sciences).

## RESULTS

### iCAR concept and iDomain screen

The LOH NOT gate targeting concept incorporating an A2 iCAR and a HER2 aCAR is illustrated in figure 1A. A screen with primary T-cells was undertaken to identify iCAR with new iDomains that efficiently controlled a second generation HER2 aCAR using a bicistronic lentiviral vector configured as shown in figure 1B. The iCAR was placed first to favor iCAR expression. The iCAR backbone consisted of a BB7.2 scFv<sup>23</sup> joined to the iDomain through a 26 amino-acid (aa) PD-1 hinge and PD1 transmembrane region (HTM). A trastuzumab derived anti-HER2 scFv with a 4-1BB co-stim was the aCAR partner in all constructs. This HER2 aCAR demonstrated high in-vivo efficacy, as a single-input CAR, in multiple NSCLC tumor models with low (1+)/normal HER2 expression<sup>4</sup> (online supplemental figure S1).

The iCAR NOT gate candidates were ranked using a luciferase cytotoxicity assay with parental H1703 A2

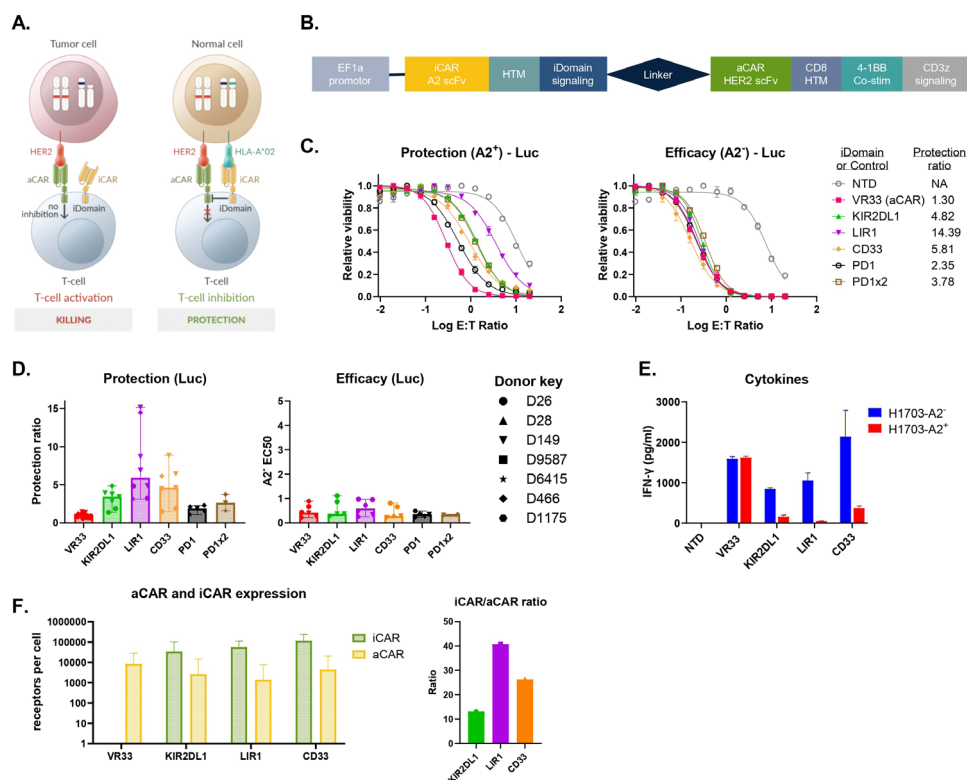


**Figure 1** Novel A2 inhibitory chimeric antigen receptor (iCAR) screen. (A) iCAR NOT gate targeting of A2 loss of heterozygosity (LOH) in lung cancer. The iCAR LOH target concept is illustrated as described in the Introduction section. (B) Bicistronic lentiviral CAR structure. The iCAR and activating CAR (aCAR) were encoded in a bicistronic lentiviral vector under control of an EF1 $\alpha$  promoter and joined by a viral T2A for the initial iDomain screen. (C) Head-to-head luciferase (Luc) killing assays. Luciferase expressing H1703-A2<sup>+</sup> or H1703-A2<sup>-</sup> target cells were treated at the indicated E:T ratios and viability was determined after 18 hours incubation. CAR-T input was adjusted according to transduction efficiency (16%–73%). Mock transduced T-cells (NTD) were utilized as a negative control and a single input HER2 aCAR was used as a positive control (VR33). The protection ratio is equal to  $A2^{+}_{EC50} / A2^{-}_{EC50}$ . (D) Replication of killing assays. The results of independent parallel luciferase killing assays with lead iDomain constructs and aCAR control were plotted in histograms. The donor key applies to all figures in this report. (E) Interferon (IFN)- $\gamma$  secretion assays. The IFN- $\gamma$  concentration in cell supernatants was determined following 18 hours coculture at E:T ratio of 5:1. IFN- $\gamma$  secretion was below detection for effector only control. (F) iCAR and aCAR expression. The cell-surface iCAR and aCAR expression level was determined by quantitative FACS.



positive (A2<sup>+</sup>) lung cancer cells to represent normal tissues, and CRISPR-edited A2 negative (A2<sup>-</sup>) cells to represent tumor LOH (online supplemental figure S1). The H1703 cell line expresses target levels (A2, 8.0E5; HER2, 2.0E4 receptors per cell) near to the median of most normal tissues, primary tumors and cancer cell lines (online supplemental table S2, online supplemental figure S3). The LIR1 iDomain emerged as the top performer in head-to head comparisons of the isolated hits based on a protection ratio (A2<sup>+</sup><sub>EC50</sub>/A2<sup>-</sup><sub>EC50</sub>) derived from parallel E:T titrations (figure 1C), and was selected for further development. However, it should be noted that the performance of LIR1 was more comparable to the KIR2DL1 and CD33 iDomains when independent assays with multiple donors were collectively analyzed (figure 1D). The killing potency among the lead candidates was not significantly different (H1703-A2<sup>-</sup>, EC<sub>50</sub> 0.3–1) (figure 1D). The LIR1, KIR2DL1 and CD33 iCAR similarly inhibited IFN-γ secretion on H1703-A2<sup>+</sup> targets (figure 1E), and these iCAR and aCAR exhibited robust coexpression although biased towards iCAR expression (figure 1F). More work is needed to understand the relative merits of the LIR1 iCAR and other iDomain constructs.

### LIR1 iCAR optimization

The LIR1 iCAR NOT gate identified in the iDomain screen (VR51) was extensively optimized with respect to the iCAR scFv, HTM and bicistronic linker. The top leads are represented schematically in figure 2A and included a highly characterized benchmarking agent (VR354) and two clinical candidates (VR428 and VR447). Changing the iCAR scFv to a particular fully human variant exhibited the greatest positive impact on H1703-A<sup>+</sup> target cell protection (online supplemental figure S2B). The VR428 iCAR with a humanized BB7.2 scFv (hzBB7.2) retained the potency and protection ratio of the benchmark (figure 2C, D). Substitution in VR447 with the fully-human anti-A2 antibody (huTNG3.2) enhanced protection about 3-fold. The potency and basal activity of the HER2 aCAR was not affected by any of the iCAR scFv changes evaluated.

The experiments summarizing the HTM optimization are presented in online supplemental figure S5. The natural LIR1 extracellular region consists of four Ig-like domains (D1–D4) totaling 433 residues followed by a 52 amino acid juxtamembrane stem.<sup>24</sup> Protection increased about eightfold when the D1–D4 Ig motifs were eliminated in VR354 suggesting that the extended

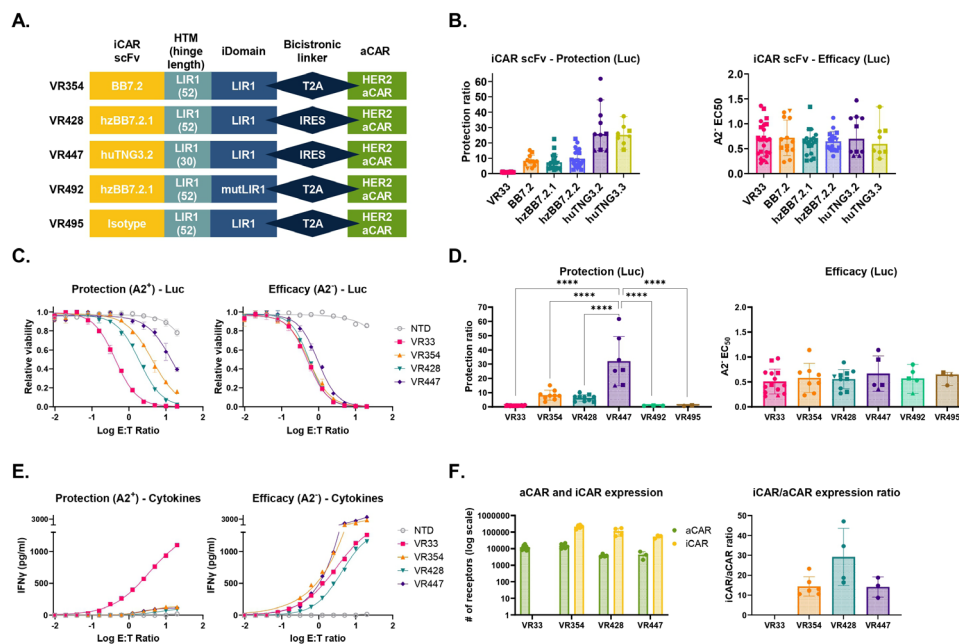


**Figure 2** Leukocyte immunoglobulin-like receptor B1 (LIR1) inhibitory chimeric antigen receptor (iCAR) optimization. (A) Diagram of iCAR NOT gate leads. The HER2 aCAR was identical as shown in figure 1B. (B) The scFv strongly affects protection. Parallel H1703 Luc killing assays were performed to evaluate different anti A2 scFv. Hinge length was 52aa for murine BB7.2, HzBB7.1, and HzBB7.2; 30aa for huTNG3.2, and 26aa for huTNG3.3. hu and hz scFv NOT gate constructs were generated with either T2A or IRES linkers which in-vitro showed no differences. The murine BB7.2 bicistronic always used a T2A linker. (C) Representative H1703 Luc killing assays for lead candidates and controls. (D) Replicate assays for LIR1 iCAR leads and VR492 (iMut) and VR495 (Isotype). The results were evaluated using the Tukey's Honest Significant Difference (HSD) test for all pairwise comparisons. Statistically significant differences are indicated on the graph, where \* $p < 0.05$ , \*\* $p < 0.01$ , \*\*\* $p < 0.001$ , \*\*\*\* $p < 0.0001$ . (E) Interferon (IFN)-γ secretion assays. The concentration of IFN-γ in 18 h cell supernatants for the Luc killing assays shown in (C) was determined. (F) iCAR and aCAR cell-surface levels. Quantitative FACS was used to estimate iCAR and aCAR level (geometric mean) and the iCAR/aCAR expression ratio was calculated. The structure-function analysis was conducted with CAR-T cells enriched by capture with PE-labeled A2 tetramers (80%–97% double positive) (online supplemental figure S4).

Ig-domain is not relevant to synthetic iCAR signaling. Higher resolution deletions in the stem region identified a hinge length of 30 amino acids as optimal for aCAR regulation. The iCAR/aCAR expression ratio in VR428 and VR447 transduced T-cells was skewed higher by incorporation of an IRES linker compared with VR354 which used a viral T2A site (figure 2F).

The IFN- $\gamma$  responses, associated with exposure of the lead candidates to H1703-A2<sup>+</sup> targets, were efficiently suppressed to near baseline indicating that iCAR activity inhibits T-cell activation in addition to killing (figure 2E). To examine the role of iCAR signaling in regulating aCAR activity on A2<sup>+</sup> target cells, we first inactivated the LIR1 iDomain by Tyr to Phe mutation of all four ITIMS (iMut, VR492). CAR-T cells expressing the LIR1 iMut did not protect H1703-A2<sup>+</sup> target cells (figure 2D). A similar result was obtained using an iCAR engineered with a non-specific scFv (Isotype, VR495). These results indicate iCAR protection depends on both A2 binding and LIR1 signaling.

### The stability and reversibility of CAR-T cell state

The kinetics of the transition from the aCAR activated 'killing' state (on) to the iCAR inhibited 'quiescent' state (off) has important implications for both tumor efficacy and organ protection. To address this question, we used cell imaging assays (Incucyte) of apoptosis (Annexin V) and cell growth-inhibition to assess durability and reversibility with H1650-A2<sup>+</sup> and H1650-A2<sup>-</sup> lung cancer cells generated by CRISPR editing (online supplemental figure S6). The expression of A2 and HER2 in H1650 cells is similar to H1703 cells (1.0E6 and 2.8E4 per cell, respectively (online supplemental table S2). H1650-A2<sup>+</sup> targets treated with antigen inexperienced VR428 and VR447 CAR-T cells were durably protected by iCAR engagement, whereas these cells were potently killed by VR33 aCAR-T cells (figure 3A, B). The kinetic assay revealed a 2–3 fold greater rate of cell killing for VR447 compared with VR428 CAR-T cells suggesting the former is more potent.

Target transfer experiments were performed as illustrated in figure 3C. The E:T ratio for the first challenge was lowered to 1.5:1 to reduce the presence of excess unstimulated cells and prevent excessive target cell death. The transfer experiments focused on VR447 CAR-T cells given its superior cytotoxic activity. As shown in figure 3D, E, VR447 CAR-T cells pretreated with H1650-A2<sup>+</sup> targets retained the ability to protect when rechallenged with the same targets, whereas the 'on to off' transition (A2<sup>-</sup> back to A2<sup>+</sup> targets) was shown to be reversible. The reciprocal experiment (H1650-A2<sup>-</sup> target rechallenge) generated results that also supported the durability and reversibility of the CAR-T cell on-off transition (figure 3F, G). The VR447 CAR-T cell killing kinetics determined with the annexin V apoptosis readout were significantly delayed compared with VR33 aCAR-T cells in the H1650-A2<sup>-</sup> challenge target cells (figure 3F). However, the delayed kinetics were much less apparent in cell killing estimates derived from the normalized growth inhibition that

incorporates apoptosis and cell replication (figure 3G). Comparable results were obtained at a twofold higher E:T challenge ratio (online supplemental figure S7).

### Modulation of CAR cell surface expression

A FACS analysis of CAR cell-surface expression with H1703-A2<sup>+</sup> or H1703-A2<sup>-</sup> targets was undertaken to evaluate intracellular receptor trafficking during the transition between the active and inactive state. The iCAR and aCAR cell-surface level was reduced after exposure of VR354 and VR428 CAR-T cells to A2<sup>+</sup> target cells (figure 4A–C). The iCAR loss was more obvious than the aCAR reduction, likely due to the high A2 antigen and iCAR expression levels. The reductions in CAR surface expression were detected within 1 hour of H1703-A2<sup>+</sup> coculture and sustained for at least 48 hours (data not shown). In contrast, coculture of VR354 and VR428 CAR-T cells with H1703-A2<sup>-</sup> target cells resulted in an approximate twofold increase in iCAR surface expression and increased aCAR expression. When VR492 CAR-T cells were cocultured with H1703-A2<sup>+</sup> target cells, the aCAR levels moderately increased and iCAR cell surface expression was reduced; however, this iCAR decrease was muted threefold to fivefold compared with the unmutated LIR1 iDomain. These data suggest that LIR1 iDomain signaling promotes the reduction of iCAR and aCAR surface expression. The more moderate reduction with VR492 CAR-T cells may be attributed to aggregation-induced internalization. The recovery of CAR cell surface expression in the absence of target cells was monitored for 6 days after transfer of VR428 CAR-T cells from H1703-A2<sup>+</sup> coculture (18 hours) to fresh growth media. The majority of cells restored CAR expression on day 2 post transfer (figure 4D). The changes in iCAR and aCAR cell surface expression described in figure 4 were also observed using other lung cancer cell lines and the KIR2DL1 and CD33 iDomains (online supplemental figure S8).

### iCAR NOT gate specificity in mixed A2<sup>+</sup>/A2<sup>-</sup> spheroids

We utilized 3D culture methods to develop homogenous and mixed A2<sup>+</sup>/A2<sup>-</sup> H1650 lung cancer spheroids to evaluate iCAR NOT gate specificity under conditions intended to represent mixed tumor LOH in-situ (figure 5A–C). There was little evidence of cell mixing at A2<sup>+</sup>/A2<sup>-</sup> interface over 120 hours (compare admix and adjacent images). The protective effect of iCAR engagement obtained using parallel 2D luciferase killing assays was replicated with homogenous RFP A2<sup>+</sup> and GFP A2<sup>-</sup> spheroids. In adjacent spheroids the NOT gate CAR-T cells differentially protected the H1650-A2<sup>+</sup> cells. In contrast, in admix spheroids, protection of H1650-A2<sup>+</sup> cells was lost. The different outcomes with adjacent and admix spheroids suggest that A2<sup>+</sup> cells may be spared when A2<sup>+</sup>/A2<sup>-</sup> tissue boundaries are distinct, whereas highly intermixed cells are collectively destroyed. The high sensitivity of all spheroid compositions to the VR33 aCAR-T cells indicates that uneven CAR-T access did not significantly contribute to the bystander effect.

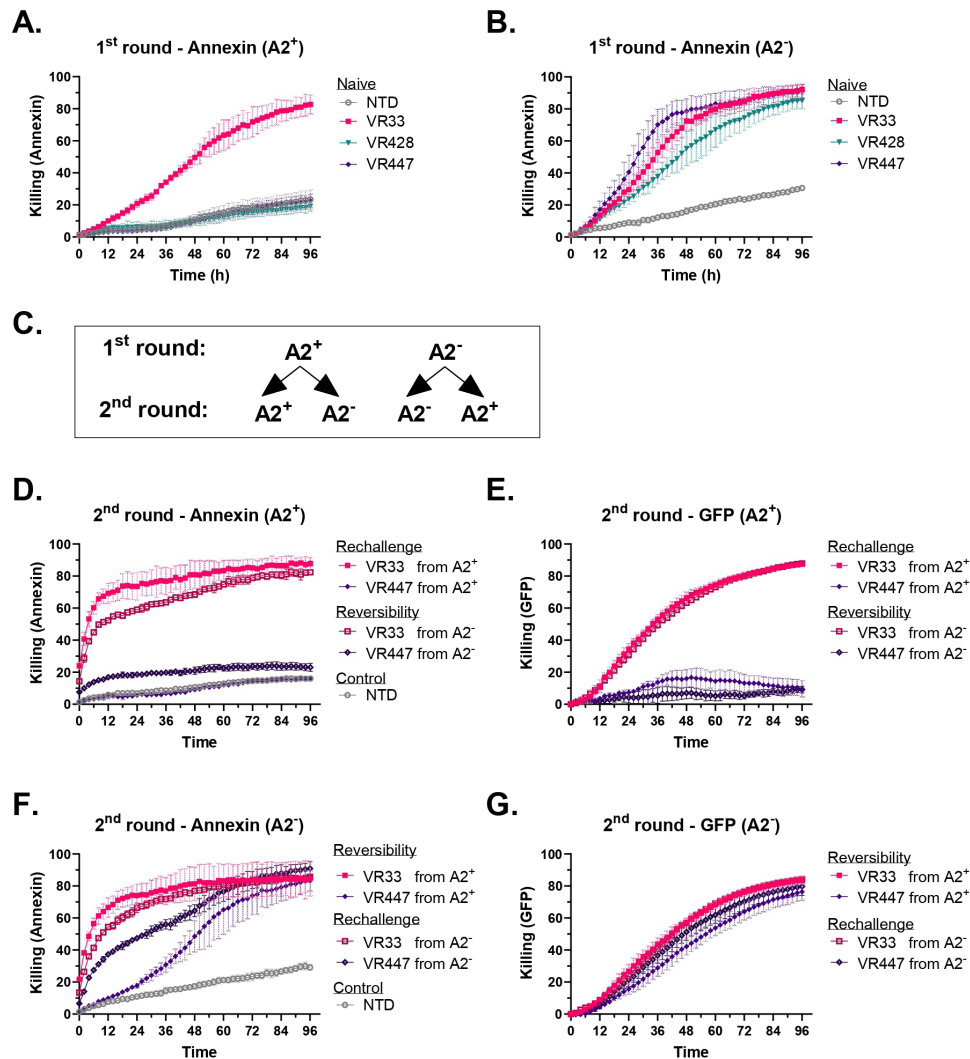


**Figure 3** Durability and reversibility of chimeric antigen receptor T (CAR-T) on-off state. (A, B) Naïve CAR-T cell targeting kinetics. Green fluorescent protein (GFP) expressing H1650-A2<sup>+</sup> and H1650-A2<sup>-</sup> cell targets were treated with naïve CAR-T or non-transduced (NTD) T-cells (E:T 3:1) as indicated. Cell death was monitored with an Incucyte Annexin-V apoptosis assay. Comparable results were obtained when cell killing was derived from growth inhibition curves. (C) Antigen exchange and repeated challenge design. CAR-T cells were cocultured with either H1650-A2<sup>+</sup> or H1650-A2<sup>-</sup> target cells (E:T 1.5:1) for 48 hours followed by transfer to either the same H1650 target cells to evaluate durability, or the opposite target cells to evaluate reversibility. (D, E) H1650-A2<sup>+</sup> 2<sup>nd</sup> round Assays. H1650-A2<sup>+</sup> or H1650-A2<sup>-</sup> pretreated CAR-T cells as indicated in the legend to each graph were applied to H1650-A2<sup>+</sup> target cells (E:T 1.5:1). (F, G) H1650-A2<sup>-</sup> second round assays. The assay described in (D, E) was repeated except the second round targets cells were H1650-A2<sup>-</sup> cells. (D, E) Annexin V readout. (E, G) Cell growth inhibition. The change in GFP<sup>+</sup> cell area was normalized to the T<sub>0</sub> value and NTD.

### Characterization of 2D bystander activity

The bystander effect with admix spheroids was also observed in 2D assays performed with H1650 targets (online supplemental figure S9). To evaluate the HER2 dependence of bystander killing, the admix studies were performed according to the scheme in figure 5D. Target elimination by VR33, VR428 and VR447 CAR-T cells in parallel assays was dependent on HER2 expression indicating that HER2 is necessary for CAR-T cell activation and killing in this context (figure 5E, parallel assays). However, significant bystander cytotoxicity was observed in the absence of HER2 expression against A2<sup>+</sup> HER2<sup>-</sup> cells in admix cultures approaching 60%–70% of VR33 aCAR-T (figure 5E, admix 2). Equivalent results were

obtained in admix experiments with A2<sup>-</sup> HER2<sup>-</sup> double negative targets ruling out involvement of A2 and the iCAR in bystander killing (online supplemental figure S10). The possibility that the bystander effect is peculiar to the H1650 cancer cell line was ruled out in an admix 2D study performed with H1703 cells (online supplemental figure S11). Bystander killing did not appear to depend on alloreactivity since the effect was recorded with nine different PBMC donors (online supplemental figure S12). Moreover, the bystander effect was observed with CAR-T cells derived from TCR null VR477 CAR-T cells generated by CRISPR editing (figure 5F). Finally, the bystander effect was also demonstrated in admix experiments with single input HER2 or CD19 aCAR, using



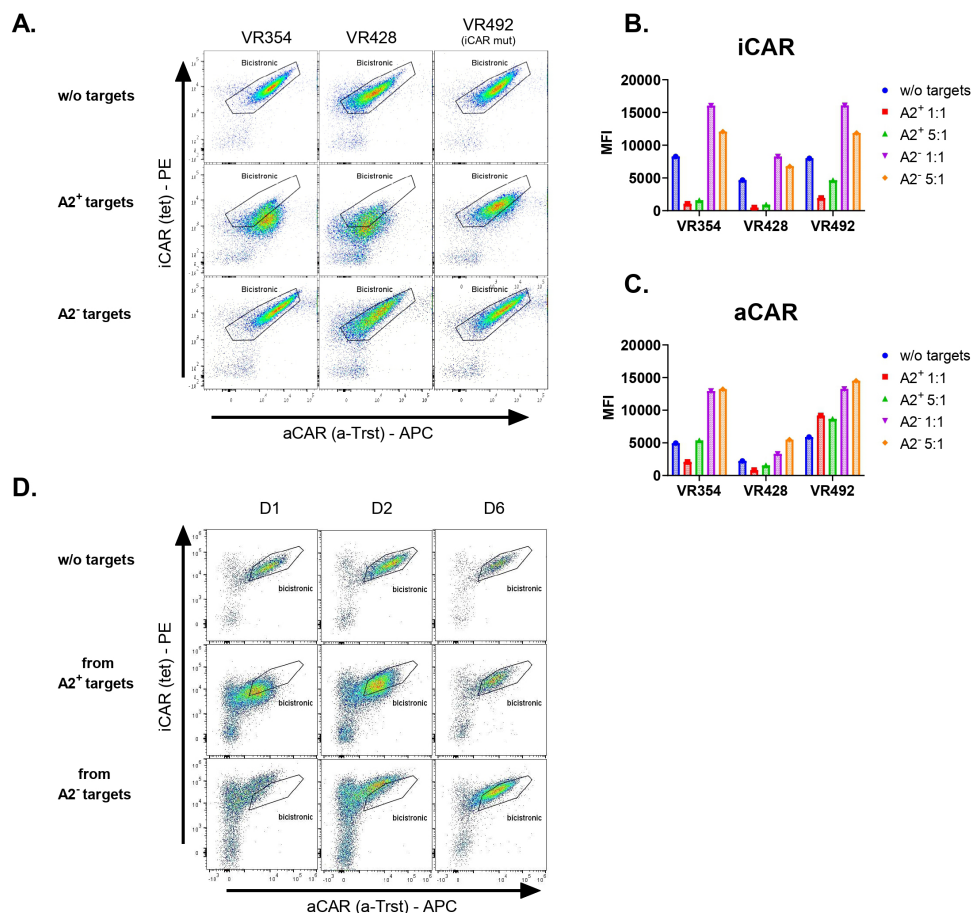


**Figure 4** Leukocyte immunoglobulin-like receptor B1 (LIR1) inhibitory signal lowers activating chimeric antigen receptor (aCAR) and inhibitory CAR (iCAR) surface expression. (A) Target cell exposure alters CAR surface levels. FACS analysis was performed using HLA-A\*02 tetramer (tet) and antitrastuzumab antibody (a-Trst) after 18 hours culture, without target coincubation, culture with H1703-A2<sup>+</sup>, or H1703-A2<sup>-</sup> target cells. The inability to detect the non-specific scFv CAR prevented parallel studies with the HLA-A2 binding deficient iCAR (VR495). (B, C) Quantitation of CAR changes. MFI values in (A) were graphed without normalization. (D) Recovery of CAR expression. VR428-CAR-T cells cocultured as indicated in (A) were separated from target cells by anti E-cadherin and anti P-cadherin selection. FACS analysis was performed on days 1, 2 and 6 after transfer to fresh growth medium supplemented with IL2.

H1650 cells engineered to express CD19, to rule out an assay artifact peculiar to a HER2 aCAR (online supplemental figure S13). Taken together, these results strongly suggest that the bystander effect has both HER2 dependent and independent components. Notably, bystander killing of HER2<sup>-</sup> targets was found to occur at a slower rate than HER2<sup>+</sup> targets.

#### NOT gate CAR-T cells eliminate A2<sup>-</sup> tumors and protect A2<sup>+</sup> tumor in-vivo

The H1703 isogenic cell lines were used to develop parallel in-vivo tumor models using NSG immunodeficient mice (figure 6A, B). H1703-A<sup>+</sup> tumors, representing 'normal tissue', were challenged with a high CAR-T dose (5.0E6 to 10E6 CAR<sup>+</sup> cells per mouse) as a stringent test for iCAR protection. H1703-A2<sup>-</sup> tumors, modeling LOH, were treated with lower CAR-T doses (1.5E6 CAR<sup>+</sup> cells) to evaluate killing potency. Over several studies, we found 1.5E6 CAR-T cells to be the lowest dose for achieving consistent tumor control with the single input

VR33 aCAR-T and iCAR NOT gate CAR-T cells (data not shown).

Cells expressing a LIR1 bicistronic lentiviral construct with murine BB7.2 scFv and PD-1 HTM (VR51) discriminated between A2<sup>+</sup> and A2<sup>-</sup> tumors at a 1.5E6 CAR-T dose, but clearance of A2<sup>+</sup> tumors was observed at the higher 5E6 CAR-T dose (online supplemental figure S15). Replacement of the PD1 HTM with an optimized LIR1 HTM and humanized/fully human scFv (VR428/VR447), together with utilization of an IRES element, enabled efficient protection at higher dosing (figure 6C, D). The CAR-T cell CD4/8 proportion was typically greater for NOT gate iCARs compared with NTD and VR33 (3.3 vs 0.5, respectively) (online supplemental figure S16). Stable vector copy number was 5.5±1.8 for VR33 and 1.1±0.5 for VR428 over the dosing interval where examined (online supplemental figure S16). The tumor growth and hCD3<sup>+</sup> T-cell counts for the individual mice after T cell treatment is shown in online supplemental figure S17. The VR33 aCAR-T cells eradicated both A2<sup>+</sup> and A2<sup>-</sup> tumors

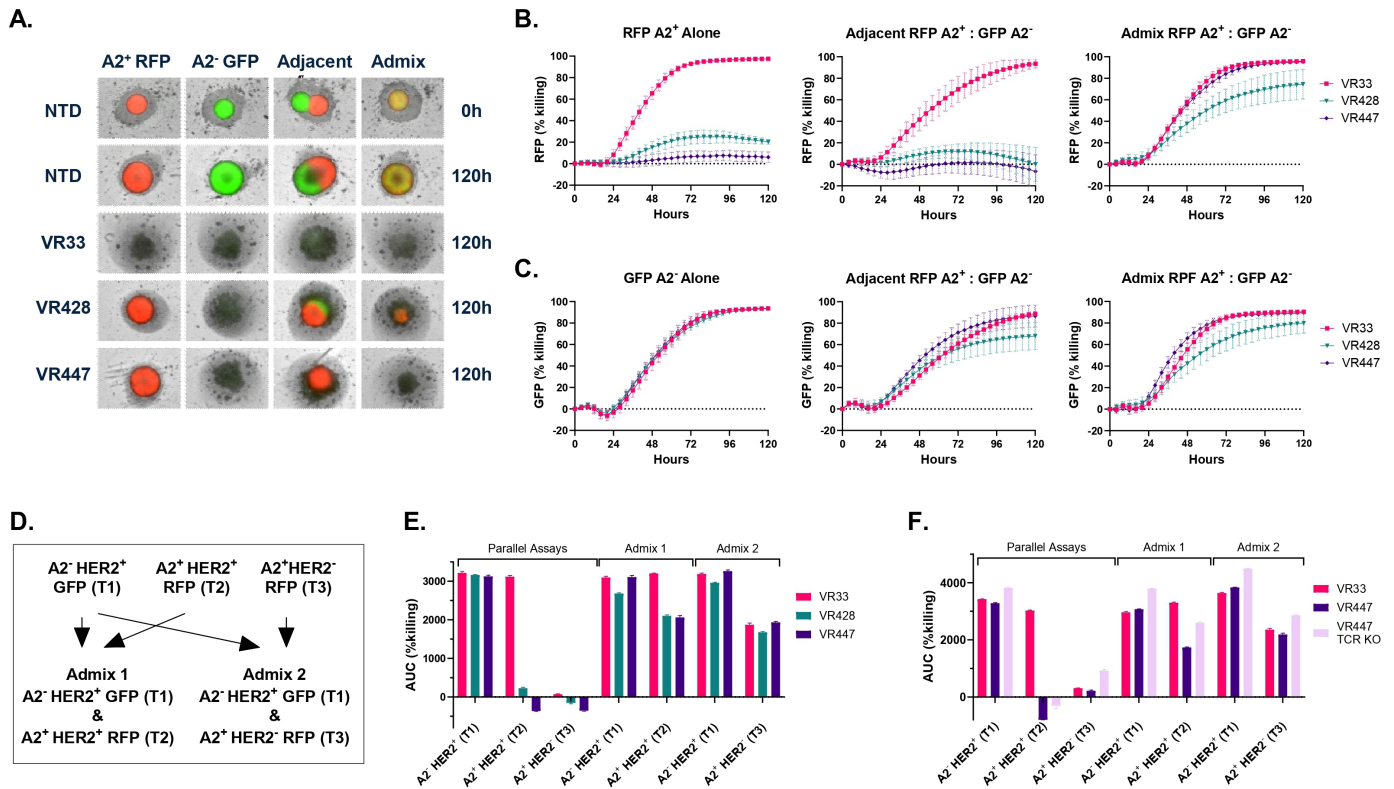


**Figure 5** Leukocyte immunoglobulin-like receptor B1 (LIR1) inhibitory chimeric antigen receptor (iCAR) NOT gate selectivity in mixed 2D and 3D cultures of A2<sup>+</sup> and A2<sup>-</sup> targets. (A) Viable imaging of representative spheroid assays. Admix spheroids were prepared by seeding H1650 targets at 1:1 ratio on low adherence plates. Adjacent spheroids were cultured separately and then combined without dissociation and the interface formed spontaneously. Assays were initiated with the addition of 5K non-transduced (NTD) or chimeric antigen receptor T (CAR-T) cells. Loss of fluorescence is associated with cell killing. (B, C) Kinetics of spheroid killing. The cytotoxic effect of CAR-T cells against RFP H1650-A2<sup>+</sup> (B) and GFP H1650-A2<sup>-</sup> spheroids (C) (n=6) was plotted after normalization to T<sub>0</sub> and NTD controls. A video is available in online supplemental video S1. (D) Design of Admix 2D culture experiments. The genotype of H1650 targets designated (T1, T2 and T3) and their respective fluorescent protein label is indicated. The adherent targets were separately treated with NTD or CAR-T cells in parallel assays. Admix experiments consisted of an equal mixture of GFP and RFP targets as indicated (E:T 4:1). (E) Evaluation of A2 and HER2 dependence of target cell killing in parallel and admix cultures. Histogram of area under the curve (AUC) for the kinetics for target cell killing relative to NTD cells for the assays identified in (D). The kinetic plots are shown in online supplemental figure S9. The results were replicated, and fluorescent labels were reversed to rule out detection bias in admix cultures (online supplemental figure S10). The rate and extent of A2<sup>+</sup> target killing in admix cultures were found to be sensitive to the A2<sup>+</sup>/A2<sup>-</sup> target cell ratio (online supplemental figure S14). (F) The bystander effect is not T-cell receptor (TCR) dependent. The killing kinetics of VR33 and VR447 CAR-T against H1650 targets was compared with VR447 CAR-T cells in which TCR was deleted by CRISPR editing (E:T 4:1).

by about 31 days post CAR-T injection indicating that both tumors are sensitive to HER2-targeted killing. The VR33 aCAR-T cell killing, with both tumor genotypes, was associated with a robust increase in serum human IFN- $\gamma$  at 7 days following T cell treatment, as well as obvious expansion of peripheral human CD3<sup>+</sup> T-cells at 14 days after T cell treatment. Similar increases in human IFN- $\gamma$  and hCD3<sup>+</sup> T-cells were associated with the control of A2<sup>-</sup> tumors in mice treated with the NOT gate CAR-T cells. However, the IFN- $\gamma$  and hCD3<sup>+</sup> T-cells markers were not increased in treated A2<sup>+</sup> tumor-bearing mice supporting the concept that iCAR-mediated protection operates through the inhibition of T-cell activation.

#### A2 knock out overcomes cis-inhibition in A2<sup>+</sup> donors

Our target expression analyses revealed that T-cells express exceptionally high levels of HLA-A that are

several fold greater than most non-hematopoietic tissues (online supplemental figure S2). FACS analysis of NOT gate CAR-T cells generated with A2<sup>+</sup> donors revealed that iCAR detection with A2 tetramers was blocked (online supplemental figure S18) raising the possibility that the iCAR was bound to A2 in a cis-configuration. The functional consequences of cis-iCAR inhibition are illustrated (figure 7A) and constitute a significant barrier to clinical translation. To evaluate the consequences of iCAR and A2 coexpression, the functional activity of VR428 transduced CAR-T cells derived from A2<sup>-</sup> and A2<sup>+</sup> donors, with and without A2 CRISPR editing, was compared using the H1703 luciferase killing assay. The guide RNA was selected to capture most known A2 sequences while minimizing activity against HLA-B/C. The ability to protect H1703-A2<sup>+</sup> target cells was fully lost, compared with A2<sup>-</sup> donors,

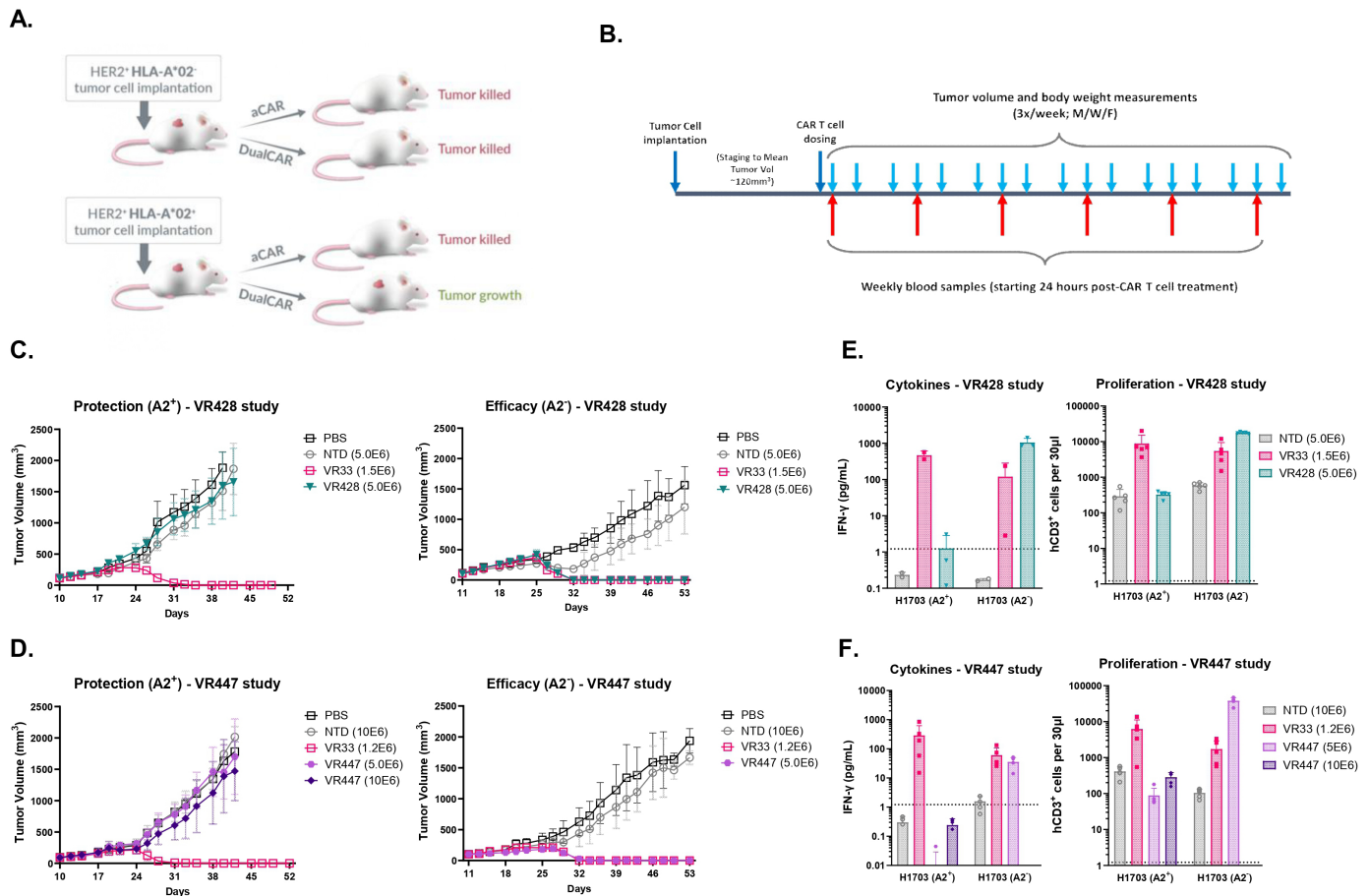


**Figure 6** In-vivo proof of concept. (A, B) Study design and endpoints. H1703-A2<sup>+</sup> or H1703-A2<sup>-</sup> cells were separately implanted into NSG mice (NOD.Cg-Prkdcscid Il2rgtm1Wjl/SzJ). chimeric antigen receptor T (CAR-T) treatments (single dose, intravenous, n=5) with test articles engineered by inhibitory CAR (iCAR) capture (>90% pure) were administered to tumor bearing mice in parallel. (C, D) Tumor growth inhibition (TGI). The ability of NOT gate CAR-T cells to distinguish A2<sup>+</sup> and A2<sup>-</sup> tumors was evaluated in independent studies. The x-axis for the TGI curves starts on the day of test article injection. (E, F) Interferon (IFN)- $\gamma$  and CAR-T cell analysis. The activation and proliferation of CAR-T cells were monitored by determining the circulating concentration of IFN- $\gamma$  (day 7 post injection) and the peripheral hCD3<sup>+</sup> T-cells counts (day 14 post injection). The time points selected were typically the peak values. Essentially, all peripheral hCD3<sup>+</sup> T-cells were found to be CAR positive (data not shown). It should be noted that in-vivo studies resolved differences in iCAR protection with T2A and IRES linkers and other features that were not resolved in-vitro. The dose of each test article is given in the legends in parentheses.

when A2<sup>+</sup> donors were used for CAR-T production (figure 7C, D) strongly suggesting that cis-binding efficiently inhibits iCAR activity. However, CRISPR editing combined with depletion of residual nonedited T-cells (online supplemental figure S19) fully restored the ability to protect H1703-A2<sup>+</sup> targets (figure 7E) suggesting a path forward for clinical process development.

## DISCUSSION

There is strong interest in improving interventions targeting normal HER2 expression based on recent clinical successes obtained with HER2 antibody drug conjugates.<sup>25 26</sup> The LIR1 NOT gate approach we have described may be useful in expanding HER2 normal targeting to a new treatment population (A2 LOH). The leukocyte Ig-like receptors, which includes LIR1, have been assigned roles in regulating innate and adaptive immunity.<sup>27</sup> The N-terminal Ig-motifs (D1 and D2)

bind HLA-I/ $\beta$ 2M class<sup>24</sup> and inhibitory signaling is mediated by ITIM tyrosine phosphorylation that recruits Src homology region 2 domain-containing phosphatase-1 (SHP-1) tyrosine phosphatase.<sup>28</sup> Our mechanistic analysis strongly suggests that the LIR1 iCAR operates by a similar mechanism since LIR1 ITIMs and A2 binding were found to be essential for protection. The alterations of CAR surface expression that we have detected on target exposure, negatively for A2<sup>+</sup> HER2<sup>+</sup> targets and positively with A2<sup>-</sup> HER2<sup>+</sup> targets, are connected to LIR1 iDomain signaling, and may be useful pharmacodynamic markers. However, higher resolution time course experiments are needed to understand how altered CAR cell trafficking may regulate the on/off state transitions.

The majority of LIR1 iCAR constructs that we have evaluated in-vivo fully protected H1703-A2<sup>+</sup> tumors at a 1.5E6 CAR-T per mouse dose. However, the VR428 and VR447 NOT gate leads were selected for further development



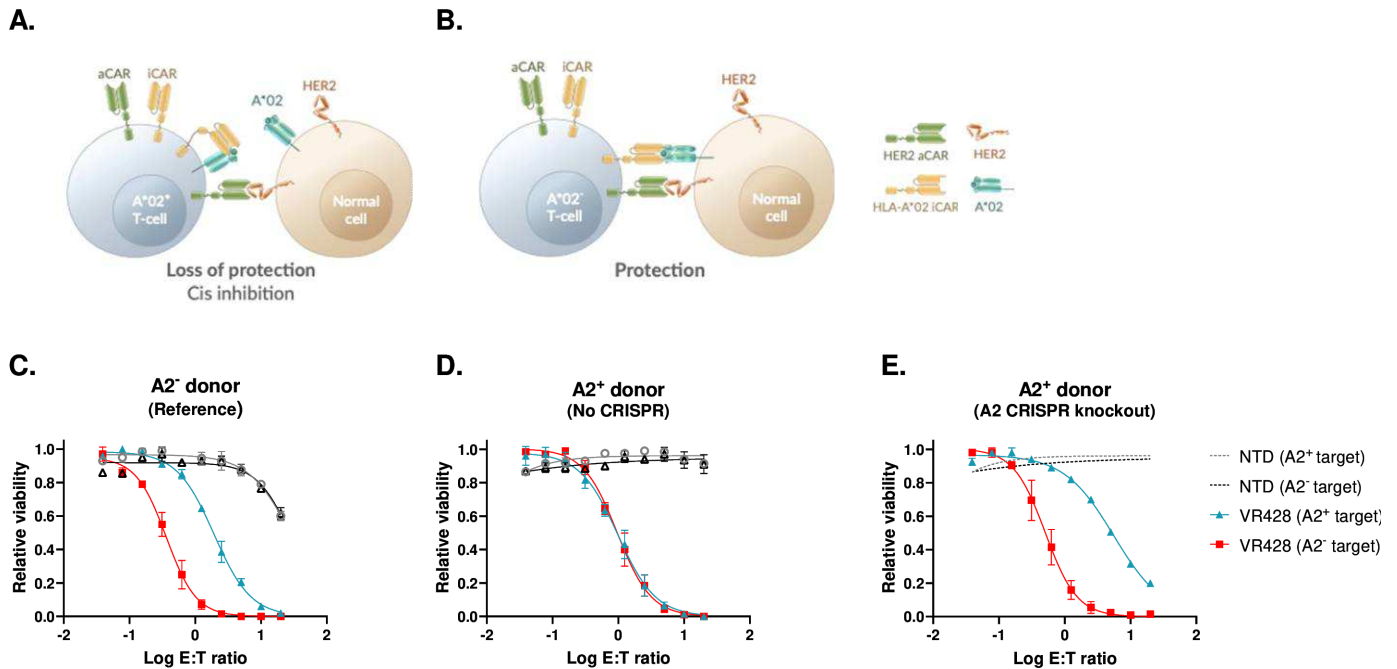


**Figure 7** A2 knockout is required in chimeric antigen receptor T (CAR-T) cells derived from A2<sup>+</sup> donors. (A) Model for loss of inhibitory CAR (iCAR) protection with autologous donors. Binding of A2 in cis-configuration autoinhibits iCAR activity and allows activating CAR (aCAR) directed killing of H1703-A2<sup>+</sup> targets. (B) Protection with allogenic A2<sup>-</sup> donors. Activation of the iCAR in trans-configuration by normal target cells inhibits T-cell activation and killing. (C) Cis-iCAR inhibition is absent in A2<sup>-</sup> donors. NOT gate CAR-T cells were generated with VR428 and assayed in the parallel luciferase killing assay with H1703-A2<sup>+</sup> and H1703-A2<sup>-</sup> cells. (D) Cis-inhibition with A2<sup>+</sup> donors neutralize protection. NOT gate CAR-T cells were generated with VR428 using A2<sup>+</sup> donor cells and the normal enrichment process. (E) Functional analysis of CRISPR-edited A2<sup>-</sup> NOT gate CAR-T cells. CRISPR editing was used to delete A2 expression in donor T-cells after lentiviral transduction. The dashed lines in (E) indicate the non-transduced (NTD) control shown in (D) run in parallel.

based on their ability to consistently protect at higher doses. Protection of H1703-A2<sup>+</sup> tumors was consistently accompanied by efficient inhibition of IFN- $\gamma$  production and T-cell expansion. This self-regulatory property, resembling the natural immune checkpoint inhibition, may translate into significant clinical benefit in regulating CRS and neurotoxicity, as well as reducing exhaustion due to excess T-cell amplification.

The NOT gate CAR-T cells exhibited strong specificity against A2<sup>-</sup> targets in adjacent spheroids designed to model the interface between clonal A2LOH foci and normal tissue or A2<sup>+</sup> territories in heterogeneous tumors. This result is consistent with the reversibility of NOT gate CAR-T cells activation that we and others have demonstrated in target transfer experiments. However, it is important to note that the bystander effect that we described in admix cultures (2D and 3D), in which A2<sup>+</sup> and A2<sup>-</sup> cells are highly intermixed, is inconsistent with previous iCAR NOT gate publications.<sup>16–18–20</sup> The ‘close’ bystander override of A2 target protection was extensively characterized using CRISPR editing and other gene modifications. Surprisingly, off-target killing in admix cultures also occurred in the absence of HER2 expression although at a slower rate than killing HER2<sup>+</sup> targets. Thus, bystander killing occurs by HER2-dependent (fast) and HER2-independent mechanisms (slower). Controlled experiments ruled out T-cell donor variability

and TCR-dependent allogenic effects as potential mechanisms, and other potential artifacts.

Our studies suggest that iCAR NOT gates can be tuned to generate bystander killing activity that may be clinically useful in addressing tumor heterogeneity rather than functioning as a simple digital switch.<sup>29</sup> A2 LOH has been described as an ‘early event’ in tumorigenesis, but it does not initiate cancers.<sup>12</sup> Bystander killing may extend the clinical benefit of A2 LOH targeting to cancers with a more intermixed phenotype (eg, epithelial-mesenchymal transition signature) and recruit local T-cells potentially leading to epitope spreading. However, the development of humanized mouse models that express human A2 and HER2 is needed to prove that the bystander effect is localized, and that exposure to normal tissues at distant sites reverses the CAR-T on-state before organ damage occurs.

**Acknowledgements** We are grateful to Gideon Gross for his guidance in developing the iCAR LOH targeting concept, Yvonne Chen, Jim Johnston, and Aaron Nelson for advice on experimental design and interpretation of results, and Prasad S. Adusumilli for input on potential clinical utility.

**Contributors** AS-Y, FJC, RLK, JY and GBA directed the research. DB, LW, JY, TK, MRW, GBA, OF, NC, ST, NB, YL, KV, CS, LL-K and AS-Y designed and performed the experiments. AS-Y and FJC had primary responsibility for writing and revisions. AS-Y and FJC are acting as guarantors.

**Funding** The authors have not declared a specific grant for this research from any funding agency in the public, commercial or not-for-profit sectors.

**Competing interests** All authors are current or former employees of ImmPACT-Bio.

**Patient consent for publication** Not applicable.

**Ethics approval** All procedures carried out in this manuscript were conducted at Covance, in compliance with the applicable laws, regulations and guidelines of the National Institutes of Health (NIH) and with the approval of Covance's Animal Care and Use Committee. Covance is an AAALAC accredited facility. All studies were run under MI 05 Subcutaneous Tumor Models For Evaluation of Test Agents: MI4586, MI4588, MI4589, MI4608, MI4730, MI4731, MI5160, MI5161, MI5401 and MI5402

**Provenance and peer review** Not commissioned; externally peer reviewed.

**Data availability statement** All data relevant to the study are included in the article or uploaded as supplementary information.

**Supplemental material** This content has been supplied by the author(s). It has not been vetted by BMJ Publishing Group Limited (BMJ) and may not have been peer-reviewed. Any opinions or recommendations discussed are solely those of the author(s) and are not endorsed by BMJ. BMJ disclaims all liability and responsibility arising from any reliance placed on the content. Where the content includes any translated material, BMJ does not warrant the accuracy and reliability of the translations (including but not limited to local regulations, clinical guidelines, terminology, drug names and drug dosages), and is not responsible for any error and/or omissions arising from translation and adaptation or otherwise.

**Open access** This is an open access article distributed in accordance with the Creative Commons Attribution Non Commercial (CC BY-NC 4.0) license, which permits others to distribute, remix, adapt, build upon this work non-commercially, and license their derivative works on different terms, provided the original work is properly cited, appropriate credit is given, any changes made indicated, and the use is non-commercial. See <http://creativecommons.org/licenses/by-nc/4.0/>.

#### ORCID iD

Adi Sharbi-Yunger <http://orcid.org/0000-0002-3909-1996>

#### REFERENCES

- Sermer D, Brentjens R. CAR T-cell therapy: full speed ahead. *Hematol Oncol* 2019;37 Suppl 1:95–100.
- Zhang Y, Li Y, Cao W, et al. Single-cell analysis of target antigens of CAR-T reveals a potential landscape of on-target, off-tumor toxicity. *Front Immunol* 2021;12.
- Morgan RA, Yang JC, Kitano M, et al. Case report of a serious adverse event following the administration of T cells transduced with a chimeric antigen receptor recognizing ErbB2. *Mol Ther* 2010;18:843–51.
- Jørgensen JT, Winther H, Askaa J, et al. A companion diagnostic with significant clinical impact in treatment of breast and gastric cancer. *Front Oncol* 2021;11:676939.
- Hernandez-Lopez RA, Yu W, Cabral KA, et al. T cell circuits that sense antigen density with an ultrasensitive threshold. *Science* 2021;371:1166–71. 10.1126/science.abc1855 Available: <https://www.science.org/doi/10.1126/science.abc1855>
- Hong M, Clubb JD, Chen YY. Engineering CAR-T cells for next-generation cancer therapy. *Cancer Cell* 2020;38:473–88.
- Labanieh L, Majzner RG, Mackall CL. Programming CAR-T cells to kill cancer. *Nat Biomed Eng* 2018;2:377–91.
- Garrido MA, Perea F, Vilchez JR, et al. Copy neutral LOH affecting the entire Chromosome 6 is a frequent mechanism of HLA class I alterations in cancer. *Cancers (Basel)* 2021;13:5046. 10.3390/cancers13205046 Available: <https://pubmed.ncbi.nlm.nih.gov/34680201/>
- Perea F, Bernal M, Sánchez-Palencia A, et al. The absence of HLA class I expression in non-small cell lung cancer correlates with the tumor tissue structure and the pattern of T cell infiltration. *Int J Cancer* 2017;140:888–99.
- Zhang X, Tang H, Luo H, et al. Integrated investigation of the prognostic role of HLA LOH in advanced lung cancer patients with immunotherapy. *Front Genet* 2022;13:1066636.
- Garrido MA, Rodriguez T, Zinchenko S, et al. HLA class I alterations in breast carcinoma are associated with a high frequency of the loss of heterozygosity at chromosomes 6 and 15. *Immunogenetics* 2018;70:647–59.
- McGranahan N, Rosenthal R, Hiley CT, et al. Allele-specific HLA loss and immune escape in lung cancer evolution. *Cell* 2017;171:1259–71.
- Gillette MA, Satpathy S, Cao S, et al. Proteogenomic characterization reveals therapeutic vulnerabilities in lung adenocarcinoma. *Cell* 2020;182:200–25.
- Zehir A, Benayed R, Shah RH, et al. Mutational landscape of metastatic cancer revealed from prospective clinical sequencing of 10,000 patients. *Nat Med* 2017;23:703.
- Montesin M, Murugesan K, Jin DX, et al. Somatic HLA class I loss is a widespread mechanism of immune evasion which refines the use of tumor mutational burden as a biomarker of checkpoint inhibitor response. *Cancer Discov* 2021;11:282–92. 10.1158/2159-8290.CD-20-0672 Available: <https://aacrjournals.org/cancerdiscovery/article/11/2/282/2772/Somatic-HLA-Class-I-Loss-Is-a-Widespread-Mechanism>
- Fedorov VD, Themeli M, Sadelain M. PD-1- and CTLA-4-based inhibitory chimeric antigen receptors (iCARs) divert off-target immunotherapy responses. *Sci Transl Med* 2013;5:215ra172.
- Tao L, Farooq MA, Gao Y. Cd19-CAR-T cells bearing a Kir/Pd-1-based inhibitory car eradicate Cd19+Hla-C1- malignant B cells while sparing Cd19+Hla-C1+ healthy B cells. *Cancers (Basel)* 2020;12:2612.
- Hwang MS, Mog BJ, Douglass J, et al. Targeting loss of heterozygosity for cancer-specific immunotherapy. *Proc Natl Acad Sci U S A* 2021;118:e2022410118. 10.1073/pnas.2022410118 Available: <https://doi.org/10.1073/pnas.2022410118>
- Richards RM, Zhao F, Freitas KA, et al. NOT-Gated Cd93 CAR T cells effectively target AML with minimized endothelial cross-reactivity. *Blood Cancer Discov* 2021;2:648–65.
- Sandberg ML, Wang X, Martin AD, et al. A carcinoembryonic antigen-specific cell therapy selectively targets tumor cells with HLA loss of heterozygosity in vitro and in vivo. *Sci Transl Med* 2022;14:eabm0306.
- Tokatlian T, Asuelime GE, Mock J-Y, et al. Mesothelin-specific CAR-T cell therapy that incorporates an HLA-Gated safety mechanism selectively kills tumor cells. *J Immunother Cancer* 2022;10:e003826.
- Hamburger AE, DiAndreth B, Cui J, et al. Engineered T cells directed at tumors with defined allelic loss. *Mol Immunol* 2020;128:298–310.
- Holmes NJ, Parham P. Enhancement of monoclonal antibodies against HLA-A2 is due to antibody bivalency. *J Biol Chem* 1983;258:1580–6.
- Chapman TL, Heikema AP, West AP, et al. Crystal structure and ligand binding properties of the D1D2 region of the inhibitory receptor LIR-1 (ILT2). *Immunity* 2000;13:727–36.
- Modi S, Jacot W, Yamashita T, et al. Trastuzumab deruxtecan in previously treated Her2-low advanced breast cancer. *N Engl J Med* 2022;387:9–20.
- Li BT, Smit EF, Goto Y. Trastuzumab deruxtecan in Her2-mutant non-small-cell lung cancer. *N Engl J Med* 2022;386:241–51.
- De Louche CD, Roghanian A, REVEW human inhibitory Leukocyte IG-like receptors: from Immunotolerance to Immunotherapy. *JCI Insight* 2022;7:e151553. 10.1172/jci.insight.151553 Available: <https://doi.org/10.1172/jci.insight.151553>
- Bellón T, Kitzig F, Sayós J, et al. Mutational analysis of immunoreceptor tyrosine-based inhibition motifs of the IG-like transcript 2 (Cd85J) leukocyte receptor. *J Immunol* 2002;168:3351–9.
- Klampatsa A, Leibowitz MS, Sun J, et al. Analysis and augmentation of the immunologic bystander effects of CAR T cell therapy in a syngeneic mouse cancer model. *Mol Ther Oncolytics* 2020;18:360–71.